

Theory of the Rydberg blockade with multiple intermediate-state excitations

P. R. Berman  and Huy Nguyen

Physics Department, University of Michigan, 450 Church Street, Ann Arbor, Michigan 48109, USA

Alberto G. Rojo

Department of Physics, Oakland University, Rochester, Michigan 48309, USA



(Received 22 February 2022; accepted 11 April 2022; published 28 April 2022)

We present a detailed theory of the Rydberg blockade, including contributions from multiple intermediate-state excitations. Two fields drive transitions between ground and Rydberg levels via an off-resonance intermediate state. Assuming a perfect blockade, we calculate the probability to excite fully symmetric collective states having either zero or one Rydberg excitation, but an arbitrary number of intermediate-state excitations. Both “bare” state and “dressed” state approaches are used for (1) constant amplitude driving fields and (2) adiabatic pulse driving fields. It is shown that a dressed state approach offers distinct advantages when multiple intermediate-state excitations occur. In the case of fixed amplitude fields, the multiple intermediate excitations can result in comblike modulated populations of *individual* states having one Rydberg excitation and $n \ll N$ intermediate-state excitations. However, when summed over *all* such state populations, most of the modulation disappears and the system is described to a good approximation by an effective two-level model. In the case of adiabatic, pulsed fields, there is no such modulation and an effective two-level model (in the dressed basis), corrected for light shifts, can be used to model the system. In addition to solving this problem using conventional methods, we show that similar results could be obtained using a form of the Holstein-Primakoff transformation.

DOI: [10.1103/PhysRevA.105.043715](https://doi.org/10.1103/PhysRevA.105.043715)

I. INTRODUCTION

As a consequence of the dipole-dipole interaction between highly excited Rydberg atoms, it is possible to suppress multiple Rydberg excitations in an atomic ensemble when the atoms are driven by optical fields. The suppression mechanism produces a “dipole or Rydberg blockade” that can be used to entangle a large number of atoms. As proposed originally by Lukin *et al.* [1], such a Rydberg blockade can be used as an important element in quantum computing and quantum information protocols. Experimental confirmation of the Rydberg blockade has been reported for both two-atom [2] and many-atom [3] systems.

In the simplest theoretical modeling of the Rydberg blockade, the ensemble of atoms is taken to consist of two collective states, the ground state and a fully symmetric state involving a single Rydberg excitation. Excitation of the collective Rydberg state is often accomplished using two-photon excitation via an off-resonant intermediate state. In the two-level model, the intermediate state does not appear explicitly in the formalism, having been adiabatically eliminated in some fashion. In such treatments, it is not clear whether or not there are multiple collective excitations of the intermediate state and to what extent off-resonant excitation of the intermediate states results in light shifts. The light shifts can modify the resonance condition for excitation of the blockade. In this paper, we fully account for multiple intermediate-state excitations.

The collective states that are excited in the Rydberg blockade can be related to Dicke states [4]. There is a vast literature

on both Dicke states and the Rydberg blockade. In a comprehensive article containing many references, Shammah *et al.* [5] reviewed the Dicke state dynamics for an ensemble of noninteracting two-level atoms. If the atoms are noninteracting, the Dicke formalism, while interesting, simply makes a theoretical analysis of the problem much more complex, since the expectation value of any physical observable for noninteracting atoms is simply N times that of a single atom. On the other hand, when the blockade is operational, the Dicke formalism offers distinct advantages, especially if decay is negligible and the field amplitudes are constant over the atomic ensemble. In that limit, the state vector describing the atomic ensemble is restricted to a limited subspace, namely, the fully symmetric Dicke states. Although there are many papers devoted to the state dynamics of the symmetric states in the Rydberg blockade [6], far fewer consider the role of intermediate-state excitations [7]. Moreover these papers often focus on the role of spontaneous decay rather than the modifications of the Rydberg dynamics in the absence of decay.

The goals of this paper are severalfold: (1) to provide formal justification for the use of the two-level approximation in the theory of the dipole blockade, (2) to examine the changes in the blockade that occur when there are multiple intermediate-state excitations, (3) to develop a dressed state theory of the blockade that can be used for both constant amplitude and adiabatic input pulses, (4) to underline the advantages of the dressed state approach, (5) to calculate the probability of the collective Rydberg population produced in the blockade as a function of pulse duration, (6) to compare

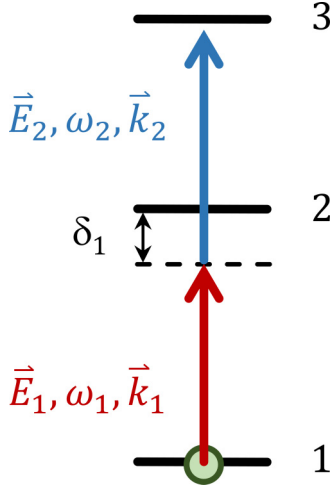


FIG. 1. Level scheme. The detuning $\delta_2 = \omega_{32} - \omega_2$ is not indicated explicitly in the figure.

this response for both constant amplitude and adiabatic input pulses, and, finally, (7) to connect our results with those that can be obtained using a form of the Holstein-Primakoff transformation [8]. We shall see that multiple intermediate-state excitations can lead to an overall modulation of the Rydberg-state population for constant amplitude fields that is absent when adiabatic pulses are used.

The paper is organized as follows: In Sec. II, the basic model is presented. A theory based on “bare” states is developed in Sec. III, allowing us to calculate the probability for excitation of the collective Rydberg state as a function of pulse duration. The analogous theory using a dressed-state basis is developed in Sec. IV for constant amplitude and adiabatic pulses. In Sec. V, a form of the Holstein-Primakoff transformation is used to reproduce the results that were obtained for adiabatic pulse excitation of the blockade.

II. GENERAL CONSIDERATIONS

Each atom is modeled as a three-level atom with lower state 1 (ground state), intermediate state 2, and upper state 3 (Rydberg level), as shown in Fig. 1. The atoms are assumed to be cold—motion of the atoms is neglected. There are two fields present:

$$\mathbf{E}_1(\mathbf{R}, t) = \frac{1}{2}E_1(t)\epsilon_1 e^{ik_1 \cdot \mathbf{R} - i\omega_1 t} + \text{c.c.}, \quad (1a)$$

$$\mathbf{E}_2(\mathbf{R}, t) = \frac{1}{2}E_2(t)\epsilon_2 e^{ik_2 \cdot \mathbf{R} - i\omega_2 t} + \text{c.c.}, \quad (1b)$$

where c.c. stands for “complex conjugate.” Field $\mathbf{E}_1(\mathbf{R}, t)$ [$\mathbf{E}_2(\mathbf{R}, t)$] has propagation vector \mathbf{k}_1 [\mathbf{k}_2], frequency $\omega_1 = k_1 c$ [$\omega_2 = k_2 c$], and polarization ϵ_1 [ϵ_2]. We define detunings

$$\delta_1 = \omega_{21} - \omega_1, \quad \delta_2 = \omega_{32} - \omega_2, \quad (2)$$

where ω_{21} is the intermediate-state to ground-state frequency and ω_{32} is the Rydberg-state to intermediate-state frequency. It is assumed that $|\delta_1| \gg |\delta_1 + \delta_2|$. In drawing the figures in this paper, we assume that $\delta_1 > 0$. Field $\mathbf{E}_1(\mathbf{R}, t)$ drives the

1-2 transition and field $\mathbf{E}_2(\mathbf{R}, t)$ drives the 2-3 transition with associated Rabi frequencies

$$\Omega_1(t) = 2\chi_1(t) = -\frac{\boldsymbol{\mu}_{12} \cdot \boldsymbol{\epsilon}_1 E_1(t)}{\hbar}, \quad (3a)$$

$$\Omega_2(t) = 2\chi_2(t) = -\frac{\boldsymbol{\mu}_{23} \cdot \boldsymbol{\epsilon}_2 E_2(t)}{\hbar}, \quad (3b)$$

where $\boldsymbol{\mu}_{12}$ and $\boldsymbol{\mu}_{23}$ are dipole matrix elements. It is assumed that both $\chi_1(t)$ and $\chi_2(t)$ are real and positive.

Two pulse amplitude envelopes are considered, square profiles having duration T for which

$$\chi_{1,2}(t) = \chi_{1,2} \Theta(t) \Theta(T - t), \quad (4)$$

where $\Theta(t)$ is a Heaviside function, and Gaussian profiles,

$$\chi_{1,2}(t) = \chi_{1,2} e^{-t^2/T_p^2}, \quad (5)$$

with

$$T_p = T/\sqrt{\pi}, \quad (6)$$

chosen such that the pulse areas of the square and Gaussian pulses are equal. For the most part, it is assumed that the detunings satisfy

$$\frac{\chi_1^2}{\delta_1^2} \ll 1, \quad \frac{\chi_2^2}{\delta_1^2}, \frac{\chi_2^2}{\delta_2^2} \ll 1, \quad (7)$$

and that

$$|\delta_1|T_p \approx |\delta_2|T_p \gg 1. \quad (8)$$

Condition (7) guarantees that the intermediate-state population of a single atom is much less than unity while condition (8) ensures that the Gaussian pulses are adiabatic.

It is assumed that the Rydberg blockade is totally functional. That is, in an ensemble of N atoms, there is at most one collective Rydberg excitation in the sample. On the other hand, there can be *several* collective intermediate-state excitations. The average number of level 2 excitations is of order

$$n_2 = \frac{N\Omega_1^2}{\delta_1^2} \ll N. \quad (9)$$

Decay of levels 2 and 3 is neglected, based on the assumptions that

$$\frac{(\chi_1^2 + \chi_2^2)}{\delta_1^2} \gamma_2 T \ll 1, \quad (10a)$$

$$\gamma_3 T \ll 1 \quad (10b)$$

where γ_j is the decay rate of state j [9]. Although decay is neglected, the light shifts, which are of order χ_1^2/δ_1 , χ_2^2/δ_1 , can modify the atomic response to the applied fields if

$$\frac{\chi_1^2 T}{|\delta_1|} \gtrsim 1 \quad \text{or} \quad \frac{\chi_2^2 T}{|\delta_1|} \gtrsim 1. \quad (11)$$

The ensemble will undergo enhanced Rabi oscillations between the ground and collective Rydberg state with rate

$$\chi_{RN} = \sqrt{N} \frac{\chi_1 \chi_2}{|\delta_1|} \equiv \frac{\Omega_{RN}}{2}. \quad (12)$$

To observe m Rabi oscillations, it is necessary that $\chi_{RN}T > m\pi$. On this time scale, the light shifts will be negligible provided that

$$\frac{\chi_1 m \pi}{\chi_2 \sqrt{N}} \ll 1, \quad \frac{\chi_2 m \pi}{\chi_1 \sqrt{N}} \ll 1. \quad (13)$$

We assume that $N \gg 1$.

III. BARE ATOM BASIS

A. Single atom

For a single atom, the wave function in a field interaction representation [10] can be written as

$$|\psi(t)\rangle = a_1|1\rangle + a_2|2\rangle e^{ik_1 \cdot \mathbf{R}_1 - i\omega_1 t} + a_3|3\rangle e^{ik_1 \cdot \mathbf{R}_1 - i\omega_1 t} \times e^{ik_2 \cdot \mathbf{R}_1 - i\omega_2 t}, \quad (14)$$

where \mathbf{R}_1 is the position of the atom. The state amplitudes evolve as

$$\dot{a}_1 = -i\chi_1(t)a_2, \quad (15a)$$

$$\dot{a}_2 = -i\chi_1(t)a_1 - i\chi_2(t)a_3 - i\delta_1 a_2, \quad (15b)$$

$$\dot{a}_3 = -i\chi_2(t)a_2 - i(\delta_1 + \delta_2)a_3, \quad (15c)$$

with initial condition, $a_1(0) = 1$. It is straightforward to solve these equations numerically. For square pulses the solution for the vector $\mathbf{a}(t) = (a_1(t), a_2(t), a_3(t))$ is

$$\mathbf{a}(t) = \exp(-i\mathbf{H}t/\hbar)\mathbf{a}(0) \quad (16)$$

where

$$\mathbf{H} = \hbar \begin{pmatrix} 0 & \chi_1 & 0 \\ \chi_1 & \delta_1 & \chi_2 \\ 0 & \chi_2 & \delta_1 + \delta_2 \end{pmatrix} \quad (17)$$

is the effective Hamiltonian in a field interaction representation.

For adiabatic Gaussian pulses, it is possible to eliminate the intermediate state using

$$a_2(t) \approx -\frac{[\chi_1(t)a_1(t) + \chi_2(t)a_3(t)]}{\delta_1} \quad (18)$$

to arrive at

$$\dot{a}_1 \approx i\frac{\chi_1(t)\chi_2(t)}{\delta_1}a_3 + i\frac{[\chi_1(t)]^2}{\delta_1}a_1, \quad (19a)$$

$$\dot{a}_3 \approx i\frac{\chi_1(t)\chi_2(t)}{\delta_1}a_1 + i\frac{[\chi_2(t)]^2}{\delta_1}a_3 - i(\delta_1 + \delta_2)a_3. \quad (19b)$$

Even though there is a very small probability for the atom to be in level 2 following the pulse, these equations give the sum of level 1 and level 3 populations equal to unity. In other words, adiabatic elimination leads to an error that is exponentially small in the parameter $|\delta_1|T_p$. This is true of any asymptotic expansion—it misses only exponentially small corrections.

There is an effective net detuning from two-photon resonance given by

$$\Delta(t) = \delta_1 + \delta_2 - \frac{[\chi_2(t)]^2}{\delta_1} + \frac{[\chi_1(t)]^2}{\delta_1} \quad (20)$$

which implies that the light shifts can be larger than or comparable with the two-photon coupling rate

$$\chi(t) = \frac{\chi_1(t)\chi_2(t)}{\delta_1}. \quad (21)$$

The light shifts can be somewhat compensated by taking a nonzero two-photon detuning, but it is impossible to compensate for the light shifts at *all* times.

B. N atoms

Once the dipole-dipole interaction between different atoms in Rydberg level 3 is included, the calculation becomes very difficult. Even if the blockade is fully functional, as we assume, there can be several level 2 excitations. There is no obvious simple way to eliminate the intermediate states, in general. In other words, there is no formal justification for considering the problem as an effective two-level problem involving the ground and collective Rydberg states.

A more formal justification begins with the neglect of Rydberg-Rydberg interactions. We assume the field amplitude is constant over the sample. Then the ensemble wave function is given simply by

$$|\psi(t)\rangle = \prod_{j=1}^N (a_1|1\rangle_j + a_2|2\rangle_j e^{ik_1 \cdot \mathbf{R}_j - i\omega_1 t} + a_3|3\rangle_j e^{ik_1 \cdot \mathbf{R}_j - i\omega_1 t} \times e^{ik_2 \cdot \mathbf{R}_j - i\omega_2 t}) \quad (22)$$

where \mathbf{R}_j is the position of the atom j . When expanded, this gives a state vector that can be written as the sum of fully symmetric orthonormal phased basis kets $|N; n, q\rangle$ that have n excitations of level 2 and q excitations of level 3, that is,

$$|N; n, q\rangle = \frac{1}{\sqrt{C_n^N C_q^{N-n}}} |S_{nq}^N\rangle, \quad (23)$$

where the $|S_{nq}^N\rangle$ are fully symmetric, *un-normalized* phased states. In other words,

$$|\psi(t)\rangle = \sum_{n,q} a_1^{N-n-q} a_2^n a_3^q |S_{nq}^N\rangle = \sum_{n,q} c_{nq}^N(t) |N; n, q\rangle, \quad (24)$$

where n and q can vary from zero to N with $n + q \leq N$. It then follows immediately that

$$c_{nq}^N = \sqrt{C_n^N C_q^{N-n}} a_1^{N-n-q} a_2^n a_3^q. \quad (25)$$

The $|N; n, 0\rangle$ are not Dicke states [4], but can be related to the Dicke states if we set $n = m_{\text{Dicke}} + N/2$ and $N = 2J_{\text{Dicke}}$. Using Eqs. (25) and (15), we obtain the evolution equations

$$\begin{aligned} \dot{c}_{nq}^N = & -i[n\delta_1 + q(\delta_1 + \delta_2)]c_{nq}^N - i\chi_1(t)\sqrt{n(N-n-q+1)} \\ & \times c_{n-1,q}^N - i\chi_1(t)\sqrt{(n+1)(N-n-q)}c_{n+1,q}^N \\ & - i\chi_2(t)\sqrt{n(q+1)}c_{n-1,q+1}^N - i\chi_2(t)\sqrt{q(n+1)}c_{n+1,q-1}^N, \end{aligned} \quad (26)$$

subject to the initial conditions

$$c_{nq}^N(0) = \delta_{n,0}\delta_{q,0}, \quad (27)$$

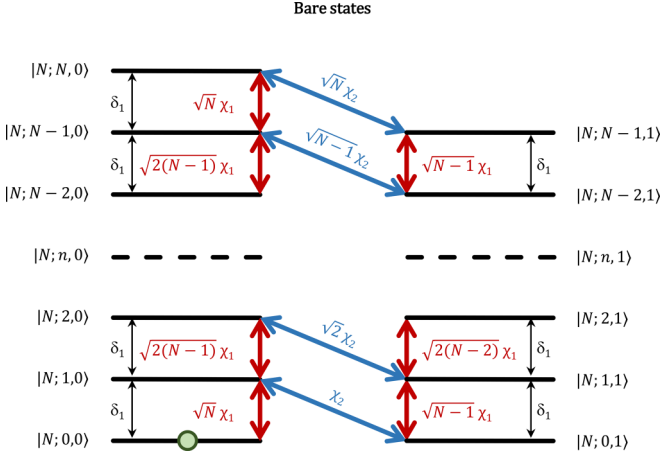


FIG. 2. Fully symmetric collective bare states. The left ladder consists of states $|N; n, 0\rangle$ containing zero Rydberg excitations and up to $n = N$ level 2 excitations. The right ladder consists of states $|N; n, 1\rangle$ containing one Rydberg excitation and up to $n = (N - 1)$ level 2 excitations. Coupling strengths are shown. Initially the atoms are in the ground state $|N; 0, 0\rangle$. The ladders are drawn for $\delta_1 + \delta_2 = 0$.

where $\delta_{i,j}$ is a Kronecker delta. Of course, for our factorized state, if you want to calculate any physical observable's expectation value, it will simply be N times the single atom expectation value.

To go from a factorized state to the blockade, we limit the values of q to be 0 or 1. Then there are two ladders of levels, the first of which has $N + 1$ steps ($q = 0$ and $0 \leq n \leq N$) and the second of which has N steps ($q = 1$ and $0 \leq n \leq N - 1$). These ladders are represented schematically in Fig. 2 for the case when $\delta_1 + \delta_2 = 0$. The equations for the state amplitudes in these two chains are

$$\begin{aligned} \dot{c}_{n0}^N &= -in\delta_1 c_{n0}^N - i\chi_1(t)\sqrt{n(N-n+1)}c_{n-1,0}^N \\ &\quad - i\chi_1(t)\sqrt{(n+1)(N-n)}c_{n+1,0}^N - i\chi_2(t)\sqrt{nc_{n-1,1}^N}, \\ \dot{c}_{n1}^N &= -i[n\delta_1 + (\delta_1 + \delta_2)]c_{n1}^N - i\chi_1(t)\sqrt{n(N-n)}c_{n-1,1}^N \\ &\quad - i\chi_1(t)\sqrt{(n+1)(N-n-1)}c_{n+1,1}^N \\ &\quad - i\chi_2(t)\sqrt{(n+1)}c_{n+1,0}^N. \end{aligned} \quad (28a)$$

$$\begin{aligned} \dot{c}_{n0}^N &= -in\delta_1 c_{n0}^N - i\chi_1(t)\sqrt{n(N-n+1)}c_{n-1,0}^N \\ &\quad - i\chi_1(t)\sqrt{(n+1)(N-n)}c_{n+1,0}^N - i\chi_2(t)\sqrt{nc_{n-1,1}^N}, \\ \dot{c}_{n1}^N &= -i[n\delta_1 + (\delta_1 + \delta_2)]c_{n1}^N - i\chi_1(t)\sqrt{n(N-n)}c_{n-1,1}^N \\ &\quad - i\chi_1(t)\sqrt{(n+1)(N-n-1)}c_{n+1,1}^N \\ &\quad - i\chi_2(t)\sqrt{(n+1)}c_{n+1,0}^N. \end{aligned} \quad (28b)$$

Field 1 produces strong coupling up and down each ladder when N is large, as is assumed. There is coupling between adjacent ladder states for n differing by 1 with a coupling constant $\sqrt{(n+1)}\chi_2$. The maximum population in each ladder occurs for $n \approx n_2/2$, where n_2 is given by Eq. (9), and approximately n_2 states are populated significantly. Thus, only the lower states of the ladders get populated in the limit that $\Omega_1^2/\delta_1^2 \ll 1$. In the case of square pulses, the solution of Eqs. (28) at time $t \leq T$ can be expressed formally as

$$\mathbf{c}_{nq}^N(t) = e^{-i\mathbf{H}_{\text{bare}}t/\hbar} \mathbf{c}_{nq}^N(0), \quad (29)$$

where \mathbf{H}_{bare} is a $(2N+1) \times (2N+1)$ matrix and \mathbf{c}_{nq}^N is a $(2N+1)$ column vector. The matrix exponential function

needs to be calculated numerically, in general. For time-dependent Rabi frequencies (pulsed fields), Eqs. (28) must be solved numerically.

If $n_2 = N\Omega_1^2/\delta_1^2 \ll 1$, it is a good approximation to include only the two lowest states of each ladder (at least two steps must be included since the lowest states of each ladder are not coupled in this bare state calculation). The truncated equations with $n \leq 1$ and $q \leq 1$ are

$$\dot{c}_{00}^N = -i\chi_1(t)\sqrt{N}c_{10}^N, \quad (30a)$$

$$\dot{c}_{10}^N = -i\delta_1 c_{10}^N - i\chi_1(t)\sqrt{N}c_{00}^N - i\chi_2(t)c_{01}^N, \quad (30b)$$

$$\dot{c}_{01}^N = -i(\delta_1 + \delta_2)c_{01}^N - i\chi_2(t)c_{10}^N - i\chi_1(t)\sqrt{N-1}c_{11}^N, \quad (30c)$$

$$\begin{aligned} \dot{c}_{11}^N &= -i(2\delta_1 + \delta_2)c_{11}^N - i\chi_1(t)\sqrt{N-1}c_{01}^N \\ &\approx -i\delta_1 c_{11}^N - i\chi_1(t)\sqrt{N-1}c_{01}^N. \end{aligned} \quad (30d)$$

For adiabatic pulses [11]

$$c_{10}^N(t) \approx -\frac{\chi_1(t)\sqrt{N}c_{00}^N(t) + \chi_2(t)c_{01}^N(t)}{\delta_1}, \quad (31a)$$

$$c_{11}^N(t) \approx -\frac{\chi_1(t)\sqrt{N-1}}{\delta_1}c_{01}^N(t), \quad (31b)$$

which, when substituted into the original equations, yield

$$\dot{c}_{00}^N \approx \frac{iN[\chi_1(t)]^2}{\delta_1}c_{00}^N + \frac{i\sqrt{N}\chi_1(t)\chi_2(t)}{\delta_1}c_{01}^N, \quad (32a)$$

$$\begin{aligned} \dot{c}_{01}^N &\approx -i(\delta_1 + \delta_2)c_{01}^N + \frac{i[\chi_2(t)]^2}{\delta_1}c_{01}^N \\ &\quad + \frac{i(N-1)[\chi_1(t)]^2}{\delta_1}c_{01}^N + \frac{i\sqrt{N}\chi_1(t)\chi_2(t)}{\delta_1}c_{00}^N. \end{aligned} \quad (32b)$$

If we let

$$c_{00}^N = \tilde{c}_{00}^N \exp\left[i\frac{N}{\delta_1} \int_{-\infty}^t [\chi_1(t')]^2 dt'\right], \quad (33a)$$

$$c_{01}^N = \tilde{c}_{01}^N \exp\left[i\frac{N}{\delta_1} \int_{-\infty}^t [\chi_1(t')]^2 dt'\right], \quad (33b)$$

then

$$d\tilde{c}_{00}^N/dt = \frac{i\sqrt{N}\chi_1(t)\chi_2(t)}{\delta_1}\tilde{c}_{01}^N, \quad (34a)$$

$$d\tilde{c}_{01}^N/dt = \frac{i\sqrt{N}\chi_1(t)\chi_2(t)}{\delta_1}\tilde{c}_{00}^N - i\Delta(t)\tilde{c}_{01}^N, \quad (34b)$$

which are the effective two-level equations, including the light shifts, with $\Delta(t)$ defined by Eq. (20).

For constant amplitude pulses and $n_2 \ll 1$, Eqs. (34) can still provide a very good approximation to the exact result provided that $\chi_2/\delta_1 \ll 1$. The solution of Eqs. (34) with constant amplitude fields is

$$|c_{01}^N(t)|^2 = \frac{4\chi_{RN}^2}{\Delta^2 + 4\chi_{RN}^2} \sin^2\left[\sqrt{\Delta^2 + 4\chi_{RN}^2}t/2\right], \quad (35a)$$

$$|c_{00}^N(t)|^2 = 1 - |c_{01}^N(t)|^2, \quad (35b)$$

where Δ is given by Eq. (20) and χ_{RN} is given by Eq. (12). With increasing χ_2/δ_1 , Eqs. (34) may fail to reproduce the

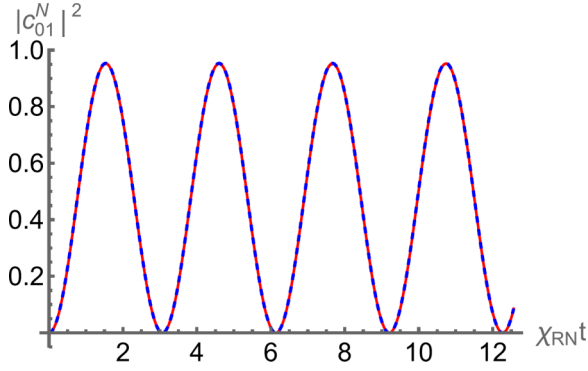


FIG. 3. Population of the lowest state of the Rydberg ladder as a function of $\chi_{RN}t$ for $\chi_1 = 1$, $\chi_2 = 10$, $\delta_1 = -\delta_2 = 1000$, and $N = 500$. The solid red curve is the exact result and the dashed blue curve is the two-level result given by Eq. (57). For these parameters the two curves overlap.

nonadiabatic effects associated with the sudden turn-on of the fields. In Figs. 3 and 4, we plot $|c_{01}^N(t)|^2$ as a function of $\chi_{RN}t$ with values of χ_1 , χ_2 , δ_1 , and δ_2 given in arbitrary units. The values chosen are $\chi_1 = 1$, $\delta_1 = 1000$, $N = 500$, and $\{\chi_2 = 10, \delta_2 = -1000\}$ (Fig. 3) or $\{\chi_2 = 500, \delta_2 = -890\}$ (Fig. 4). For $\chi_2/\delta_1 = 0.01$, the exact [obtained from Eq. (29)] and “adiabatic” results are in good agreement, but for $\chi_2/\delta_1 = 0.5$, $|c_{01}^N(t)|^2$ is modulated at frequency δ_1 , even though the two-level approximation remains valid. We shall see that this nonadiabatic behavior persists for the total Rydberg population when the two-level approximation is no longer valid. The oscillation frequency in Fig. 4 is much larger than the collective Rabi frequency owing to the large light shift associated with field 2.

IV. DRESSED ATOM BASIS

A. Constant amplitude dressed states

It turns out there can be some significant advantages if (semiclassical) dressed states are used [10]. In this subsection we consider constant amplitude fields, but it turns out that adiabatic dressed states, to be discussed in the following

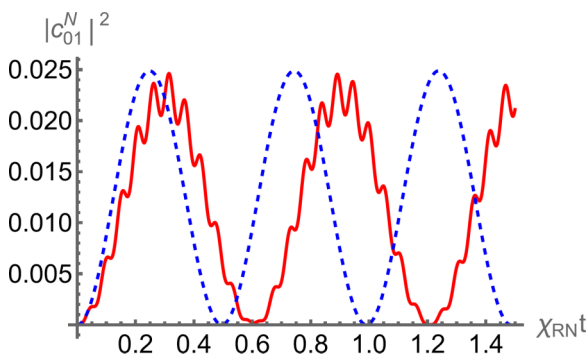


FIG. 4. Population of the lowest state of the Rydberg ladder as a function of $\chi_{RN}t$ for $\chi_1 = 1$, $\chi_2 = 500$, $\delta_1 = 1000$, $\delta_2 = -890$, and $N = 500$. The solid red curve is the exact result and the dashed blue curve is the two-level result given by Eq. (57).

subsection, may be more useful. The equations of motion for the bare state amplitudes in the absence of field 2 are

$$\dot{a}_1 = -i\chi_1 a_2, \quad (36a)$$

$$\dot{a}_2 = -i\chi_1 a_1 - i\delta_1 a_2, \quad (36b)$$

which implies an effective Hamiltonian

$$\mathbf{H}_2 = \hbar \begin{pmatrix} 0 & \chi_1 \\ \chi_1 & \delta_1 \end{pmatrix}. \quad (37)$$

We diagonalize this Hamiltonian and obtain eigenvalues

$$E_{I,II} = \hbar\omega_{I,II} = \hbar \left[\frac{\delta_1}{2} \mp \frac{\Omega}{2} \right], \quad (38)$$

where

$$\Omega = \sqrt{\delta_1^2 + 4\chi_1^2}. \quad (39)$$

The corresponding eigenkets are

$$|I\rangle = \cos\theta|1\rangle + \sin\theta|2\rangle, \quad (40a)$$

$$|II\rangle = \cos\theta|2\rangle - \sin\theta|1\rangle, \quad (40b)$$

with

$$\cos\theta = \frac{\chi_1}{\sqrt{\chi_1^2 + \omega_I^2}}, \quad (41a)$$

$$\sin\theta = \frac{\omega_I}{\sqrt{\chi_1^2 + \omega_I^2}}. \quad (41b)$$

Note that for $\chi_1^2/\delta_1^2 \ll 1$,

$$\cos\theta \approx 1 - \frac{\chi_1^2}{2\delta_1^2}, \quad (42a)$$

$$\sin\theta \approx -\frac{\chi_1}{\delta_1}, \quad (42b)$$

$$\omega_I \approx -\frac{\chi_1^2}{\delta_1}. \quad (42c)$$

The bare and dressed state amplitudes are related by

$$a_1 = \cos\theta a_I + \sin\theta a_2, \quad (43a)$$

$$a_{II} = \cos\theta a_2 - \sin\theta a_1, \quad (43b)$$

$$a_1 = \cos\theta a_I - \sin\theta a_{II}, \quad (43c)$$

$$a_2 = \cos\theta a_{II} + \sin\theta a_1, \quad (43d)$$

and the initial condition for the dressed state amplitudes is

$$a_I(0) = \cos\theta, \quad a_{II}(0) = -\sin\theta. \quad (44)$$

It is now possible to introduce symmetric collective states as before. The ensemble wave function is given simply by

$$|\psi(t)\rangle = \prod_{j=1}^N (a_I|I\rangle_j + a_{II}|II\rangle_j) e^{i\mathbf{k}_1 \cdot \mathbf{R}_j - i\omega_1 t} + a_3|3\rangle_j \\ \times e^{i\mathbf{k}_1 \cdot \mathbf{R}_j - i\omega_1 t} e^{i\mathbf{k}_2 \cdot \mathbf{R}_j - i\omega_2 t}, \quad (45)$$

where

$$|I\rangle_j = \cos\theta|1\rangle_j + \sin\theta|2\rangle_j, \quad (46a)$$

$$|II\rangle_j = \cos\theta|2\rangle_j - \sin\theta|1\rangle_j. \quad (46b)$$

When expanded, this gives a state vector that can be written as the sum of fully symmetric orthonormal dressed basis kets $|\widetilde{N}; n, q\rangle$ that have n excitations of state II and q excitations of level 3, that is,

$$|\widetilde{N}; n, q\rangle = \frac{1}{\sqrt{C_n^N C_q^{N-n}}} |\widetilde{S}_{nq}^N\rangle \quad (47)$$

where the $|\widetilde{S}_{nq}^N\rangle$ are the fully symmetric, *un-normalized* states. In other words,

$$\begin{aligned} |\psi(t)\rangle &= \sum_{n,q} a_1^{N-n-q} a_{II}^n a_3^q |\widetilde{S}_{nq}^N\rangle \\ &= \sum_{n,q} c_{nq}^{Nd}(t) |\widetilde{N}; n, q\rangle, \end{aligned} \quad (48)$$

where n and q can vary from zero to N with $n + q \leq N$. It then follows immediately that

$$c_{nq}^{Nd} = \sqrt{C_n^N C_q^{N-n}} a_1^{N-n-q} a_{II}^n a_3^q. \quad (49)$$

Using Eqs. (43) and (15), one can show that the single atom dressed state amplitudes obey the evolution equations

$$\dot{a}_I = -i\omega_I a_I - i\chi_2 \sin\theta a_3, \quad (50a)$$

$$\dot{a}_{II} = -i\omega_{II} a_{II} - i\chi_2 \cos\theta a_3, \quad (50b)$$

$$\dot{a}_3 = -i(\delta_1 + \delta_2) a_3 - i\chi_2 \cos\theta a_{II} - i\chi_2 \sin\theta a_I, \quad (50c)$$

from which it follows that the collective state amplitudes obey

$$\begin{aligned} \dot{c}_{nq}^{Nd} &= -i[(N-q)\omega_I + n\Omega + q(\delta_1 + \delta_2)] c_{nq}^{Nd} \\ &\quad - i\chi_2 \sin\theta \sqrt{(q+1)(N-n-q)} c_{n,q+1}^{Nd} \\ &\quad - i\chi_2 \sin\theta \sqrt{q(N-n-q+1)} c_{n,q-1}^{Nd} \\ &\quad - i\chi_2 \cos\theta \sqrt{n(q+1)} c_{n+1,q-1}^{Nd} \\ &\quad - i\chi_2 \cos\theta \sqrt{q(n+1)} c_{n+1,q-1}^{Nd}, \end{aligned} \quad (51)$$

where we have used the relation $\omega_{II} - \omega_I = \Omega$.

Redefining the zero of energy by setting

$$c_{nq}^{Nd}(t) = b_{nq}^{Nd}(t) e^{-iN\omega_I t} e^{-in\Omega t}, \quad (52)$$

we find, for a perfect blockade, that the needed equations are

$$\dot{b}_{n0}^{Nd} = -i\chi_2 \sin\theta \sqrt{(N-n)} b_{n1}^{Nd} - i\chi_2 e^{i\Omega t} \cos\theta \sqrt{nb_{n-1,1}^{Nd}}, \quad (53a)$$

$$\begin{aligned} \dot{b}_{n1}^{Nd} &= -i(\delta_1 + \delta_2 - \omega_I) b_{n1}^{Nd} - i\chi_2 \sin\theta \sqrt{N-n} b_{n0}^{Nd} \\ &\quad - i\chi_2 \cos\theta e^{-i\Omega t} \sqrt{n+1} b_{n+1,0}^{Nd}. \end{aligned} \quad (53b)$$

The situation has changed dramatically from the bare basis (see Fig. 5, drawn for $\delta_1 + \delta_2 = 0$). Having used a dressed basis, there is no longer any *direct* coupling up and down each of the ladders. Most of the coupling is between *adjacent* states of the two ladders having the *same* n and this coupling is

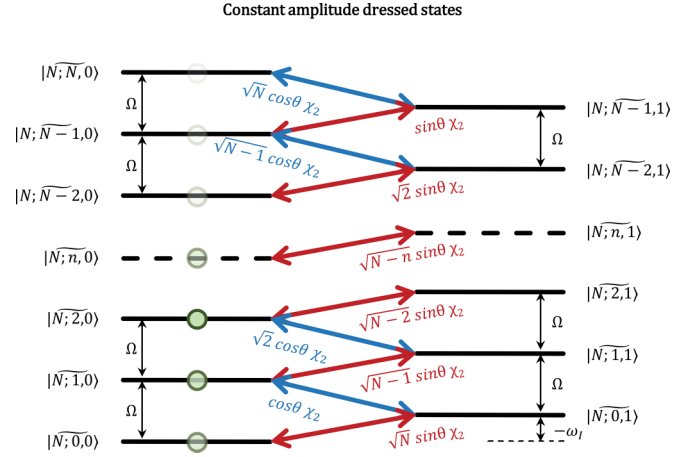


FIG. 5. Fully symmetric collective dressed states for constant amplitude fields when $\delta_1 + \delta_2 = 0$. In contrast to the bare state ladders, there is no longer any direct coupling up and down the ladders. However, initially there is now population in each of the states in the left ladder (represented by the shaded circles), with the relative populations determined from Eq. (56).

enhanced by a factor of \sqrt{N} for low-lying states if $N \gg 1$. Note that the energy of state $|\widetilde{N}; n, 0\rangle$ is lower than that of state $|\widetilde{N}; n, 1\rangle$ by $-\hbar\omega_1$, which is the *ground-state light shift associated with the first field* (recall that $-\omega_1 \approx \chi_1^2/\delta_1 > 0$). In other words the dressed states automatically include this light shift. In addition there is coupling of order $\chi_2 \sqrt{n}$ between states in different ladders differing in n by 1. Since these states are separated in frequency by $\Omega \approx \delta_1 \gg \chi_2$, this coupling leads to contributions to state amplitudes of order $\chi_2 \sqrt{n}/\Omega$.

If the χ_2 coupling between states differing in n by 1 is neglected, the problem reduces to a number of independent two state problems between different ladder states having the same n . In this limit, and in the limit that

$$|\sigma| = |\delta_1 + \delta_2 - \omega_I| \ll \chi_2 |\sin\theta| \sqrt{(N-n)}, \quad (54)$$

the approximate solution of Eqs. (53) is

$$[b_{n0}^{Nd}(t)]^{(0)} = b_{n0}^{Nd}(0) \cos[\chi_2 t \sin\theta \sqrt{(N-n)}], \quad (55a)$$

$$[b_{n1}^{Nd}(t)]^{(0)} = -ib_{n0}^{Nd}(0) \sin[\chi_2 t \sin\theta \sqrt{(N-n)}], \quad (55b)$$

where

$$\begin{aligned} b_{nq}^{Nd}(0) &= \sqrt{C_n^N} a_1^{N-n}(0) a_{II}^n(0) \delta_{q,0} \\ &= \sqrt{C_n^N} \cos^{N-n} \theta [-\sin\theta]^n \delta_{q,0}. \end{aligned} \quad (56)$$

For $\theta \ll 1$ and $N \gg n$, $|b_{n0}^{Nd}(0)|^2$ approaches a Poisson distribution having average value $\langle n \rangle = N\chi_1^2/\delta_1^2 = n_2/4$. Good convergence is achieved if a maximum of $n_2/2$ steps in each ladder is included. We have reduced the number of states from what was needed in the bare state basis by a factor of 2; moreover, we now have an approximate analytic solution.

We can improve upon this solution by using a truncated subspace for the amplitudes:

$$\mathbf{b}_n^{Nd} = [b_{n0}^{Nd}, b_{n1}^{Nd}, \tilde{b}_{n+1,0}^{Nd}, \tilde{b}_{n+1,1}^{Nd}, \tilde{b}_{n-1,0}^{Nd}, \tilde{b}_{n-1,1}^{Nd}].$$

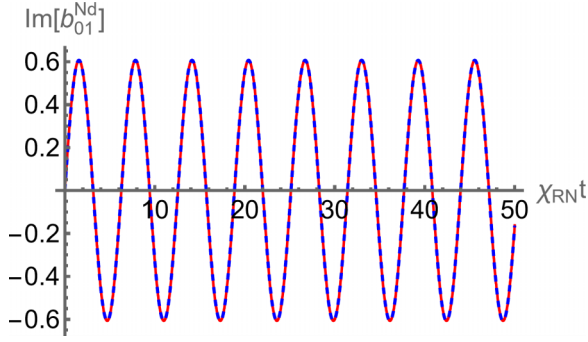


FIG. 6. Imaginary part of the amplitude associated with the lowest level of the Rydberg ladder as a function of $\chi_{RN}t$ for $\chi_1 = \chi_2 = 1$, $\delta_1 = -\delta_2 = 100$, $N = 10000$. The exact (solid red curve) and approximate solutions given by Eq. (58b) (dashed blue curve) overlap.

As is shown in the Appendix, whenever the inequalities

$$\frac{\chi_1^2}{\delta_1^2} \ll 1, \quad \frac{\chi_2}{\delta_1} \ll 1, \quad N \gg n, \quad \chi_{RN} \gg \left| \delta_1 + \delta_2 + \frac{\chi_1^2}{\delta_1} \right| \quad (57)$$

hold, approximate solutions for the dressed state amplitudes are

$$b_{n0}^{Nd}(t) \approx b_{n0}^{Nd}(0)e^{-ist} \cos(\chi_{RN}t), \quad (58a)$$

$$b_{n1}^{Nd}(t) \approx ib_{n0}^{Nd}(0)e^{-ist} \sin(\chi_{RN}t), \quad (58b)$$

where

$$s = \frac{\chi_1^2}{2\delta_1} - \frac{\chi_2^2}{2\delta_1} + \frac{\delta_1 + \delta_2}{2} = \frac{\Delta}{2}. \quad (59)$$

To this order, the solution depends on n only through the initial conditions. A somewhat improved approximation can be obtained by using the exact solution for the truncated subspace given by Eq. (A6) in the Appendix. There are no collective light shifts, proportional to N , that enter the solution.

Some illustrative plots are given for $\text{Im} b_{01}^{Nd}$ as a function of $\chi_{RN}t$ for $\delta_1 = -\delta_2$. In Fig. 6, $\chi_1 = \chi_2 = 1$, $\delta_1 = 100$, $N = 10000$, and $n = 0$. For these parameters, $n_2 = 4$ and only the first two steps in each dressed state ladder are populated significantly. Moreover, $s = 0$, such that $\text{Re} b_{01}^{Nd} \approx 0$. The solid red curve is the exact solution and the dashed blue curve, which virtually coincides with the exact solution, is the approximate solution given by Eq. (58b). Modifications of the transition amplitude introduced by light shifts can be seen in Fig. 7, in which $\chi_1 = 2$, $\chi_2 = 1$, $\delta_1 = 50$, $N = 100$, and $n = 0$. For these parameters, $s = 0.03$ and the light shifts lead to a modulation of the collective Rabi oscillations, but the exact and approximate solutions for both $\text{Im} b_{01}^{Nd}$ and $\text{Re} b_{01}^{Nd}$ (not shown) still are in excellent agreement. For larger values of χ_2/δ_1 , the approximate expression given by Eq. (58b) begins to breakdown for two reasons. There are corrections *within* the truncated subspace of order χ_2/δ_1 and there is coupling between the truncated subspaces as well. This feature is illustrated in Fig. 8, in which $\chi_1 = 2$, $\chi_2 = 30$, $\delta_1 = 50$, $N = 100$, and $n = 0$. The dotted black curve is an improved

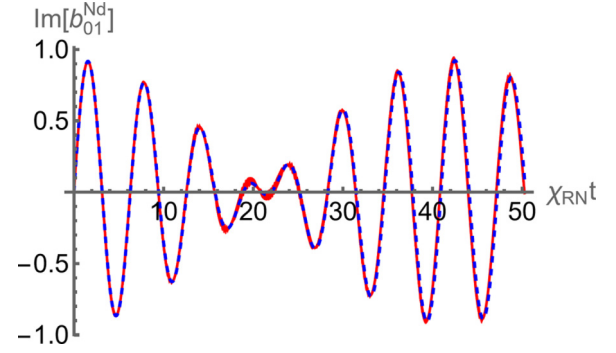


FIG. 7. Imaginary part of the amplitude associated with the lowest level of the Rydberg ladder as a function of $\chi_{RN}t$ for $\chi_1 = 2$, $\chi_2 = 1$, $\delta_1 = -\delta_2 = 50$, $N = 100$. The exact (solid red curve) and approximate solutions given by Eq. (58b) (dashed blue curve) begin to deviate from one another for large times.

approximation for $\text{Im} b_{01}^{Nd}$ in the truncated subspace given by Eq. (A6) of the Appendix.

Having derived approximate expressions for the dressed state amplitudes, we can use these results to obtain approximate expressions for the bare state amplitudes. From Eqs. (25), (43), and (49), it follows that the bare state amplitudes $c_{n0}^N(t)$ and $c_{n1}^N(t)$ can be expressed in terms of the dressed state solutions as

$$c_{n0}^N(t) = \sum_{\mu=0}^{N-n} \sum_{\nu=0}^n \sqrt{\frac{C_n^N}{C_{n+\mu-\nu}^N}} C_\mu^{N-n} C_\nu^n (-1)^\mu (\cos \theta)^{N-\mu-\nu} \times (\sin \theta)^{\mu+\nu} e^{-i(n+\mu-\nu)\Omega t} e^{-iN\omega t} b_{n+\mu-\nu,0}^{Nd}(t), \quad (60a)$$

$$c_{n1}^N(t) = \sum_{\mu=0}^{N-n-1} \sum_{\nu=0}^n \sqrt{\frac{N-n}{N-n-\mu+\nu}} \sqrt{\frac{C_n^N}{C_{n+\mu-\nu}^N}} C_\mu^{N-1-n} \times C_\nu^n (-1)^\mu e^{-iN\omega t} (\cos \theta)^{N-1-\mu-\nu} (\sin \theta)^{\mu+\nu} \times e^{-i(n+\mu-\nu)\Omega t} b_{n+\mu-\nu,1}^{Nd}(t). \quad (60b)$$

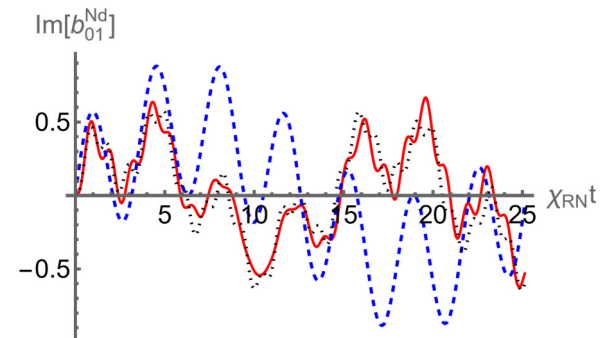


FIG. 8. Imaginary part of the amplitude associated with the lowest level of the Rydberg ladder as a function of $\chi_{RN}t$ for $\chi_1 = 2$, $\chi_2 = 30$, $\delta_1 = -\delta_2 = 50$, $N = 100$. The exact (solid red curve) and approximate solutions given by Eq. (58b) (dashed blue curve) no longer agree. The black dotted solution is an approximate solution in the truncated subspace described in the Appendix.

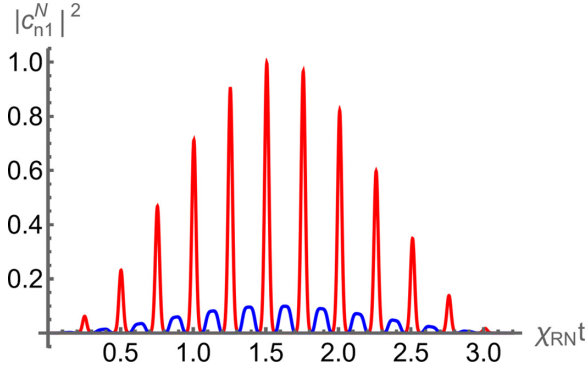


FIG. 9. Graph of $|c_{n1}^N(t)|^2$ as a function of $\chi_{RN}t$ for $\chi_1 = \chi_2 = 1$, $\delta_1 = -\delta_2 = 50$, $N = 10\,000$, and $n = 0$ (large red spikes) and 16 (smaller blue peaks).

In the limit of large N , Eqs. (60), (58), and (56) can be combined to give the approximate solutions

$$c_{n0}^N(t) \approx \sqrt{C_n^N} (1 - e^{i\Omega t})^n (-1)^n e^{-in\Omega t} \cos^n \theta \sin^n \theta e^{-iN\omega t} \times (\cos^2 \theta + e^{-i\Omega t} \sin^2 \theta)^{N-n} e^{-ist} \cos[\chi_2 t \sin \theta \sqrt{N}], \quad (61a)$$

$$c_{n1}^N(t) \approx -i \sqrt{C_n^N} (1 - e^{i\Omega t})^n (-1)^n e^{-in\Omega t} \cos^{n+1} \theta \sin^n \theta e^{-iN\omega t} \times (\cos^2 \theta + e^{-i\Omega t} \sin^2 \theta)^{N-1-n} e^{-ist} \sin[\chi_2 t \sin \theta \sqrt{N}]. \quad (61b)$$

If $\theta \ll 1$, we find

$$|c_{n0}^N(t)|^2 \approx C_n^N \left(\frac{2\chi_1^2}{\delta_1^2}\right)^n [1 - \cos(\delta_1 t)]^n \times \exp\left[-2(N-n)\frac{\chi_1^2}{\delta_1^2} [1 - \cos(\delta_1 t)]\right] \cos^2(\chi_{RN}t), \quad (62a)$$

$$|c_{n1}^N(t)|^2 \approx C_n^N \left(\frac{2\chi_1^2}{\delta_1^2}\right)^n [1 - \cos(\delta_1 t)]^n \times \exp\left[-2(N-n-1)\frac{\chi_1^2}{\delta_1^2} [1 - \cos(\delta_1 t)]\right] \times \sin^2(\chi_{RN}t). \quad (62b)$$

For $2N\chi_1^2/\delta_1^2 > 1$, the probabilities consist of a number of spikes under the envelope of the collective Rabi oscillations. For $n \ll 2N\chi_1^2/\delta_1^2$, the spikes are centered near $\delta_1 t = 2m\pi$, for integer m , but for $n \gg 2N\chi_1^2/\delta_1^2$, they are centered at $\delta_1 t = (2m+1)\pi$. This feature is seen in Fig. 9 where $|c_{n1}^N|^2$ is plotted as a function of $\chi_{RN}t$ for $\chi_1 = \chi_2 = 1$, $\delta_1 = -\delta_2 = 50$, $N = 10\,000$, and $n = 0, 16$.

In a typical experiment there is a readout pulse following the excitation pulses applied at a time where all intermediate-state populations have decayed. For large N , it is a fairly good approximation to assume that all the decay is confined to the fully symmetric states, provided the number of excited states $n_2 \ll N$ [12]. In that limit, the observed signal is proportional to the total Rydberg population P_R following the excitation

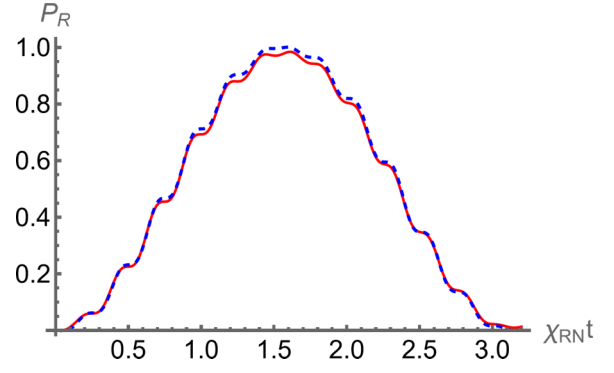


FIG. 10. Graph of the total Rydberg population $P_R(t)$ as a function of $\chi_{RN}t$ for $\chi_1 = \chi_2 = 1$, $\delta_1 = -\delta_2 = 50$, and $N = 10\,000$. The exact (solid red curve) and approximate solutions from Eq. (64) (dashed blue curve) are shown.

pulse given by

$$P_R = \sum_{n=0}^{N-1} |c_{n1}^N(t)|^2 \approx \sin^2(\chi_{RN}t). \quad (63)$$

In some sense, this is a justification for the two-level approximation that is used to model this system. However, Eq. (63) is valid only when inequalities (57) hold. In the Appendix, it is shown that an approximate solution giving first-order corrections in χ_2/δ_1 is [15]

$$P_R \approx \sin^2(\chi_{RN}t) - \frac{\chi_{RN}}{\delta_1} \sin(\delta_1 t) \sin(2\chi_{RN}t), \quad (64)$$

assuming that $\delta_1 \gg \chi_{RN}$. Most of the modulation seen in Fig. 9 is now gone, but there remains a small component of the signal which is modulated at frequency δ_1 . This modulation can be seen in Fig. 10.

B. Adiabatic dressed states

As long as $|\delta_1 T_p| \gg 1$ for the Gaussian pulse envelope of Eq. (5), we can use time-dependent adiabatic dressed states defined as in Eqs. (43), but with time-dependent $\theta(t)$. The evolution equations will be given by Eq. (51), if Ω , θ , and χ_2 are replaced by their time-dependent values, provided terms of order $\theta(t) \approx |\delta_1 T_p| \ll 1$ can be neglected. The use of adiabatic dressed states changes things dramatically since the only adiabatic dressed state that is occupied at $t = -\infty$ is the $n = q = 0$ state (see Fig. 11). As time evolves the ensemble stays mainly in the lowest state of each ladder, with a contribution to the light shifts from the first excited state of each ladder. Thus, we get an excellent approximation to the exact result by considering only the two lowest states of each ladder (or even just the lowest states, with the second states adiabatically eliminated). Moreover, following the pulse, all amplitudes except c_{00}^{Nd} and c_{01}^{Nd} go to zero. The adiabatic solution is generally valid for smooth pulses, provided

$$\Omega(t)T_p = \sqrt{\delta_1^2 + [\chi_1(t)]^2} T_p \gg 1; \quad (65)$$

that is, it is not restricted to values $[\chi_1(t)]^2/\delta_1^2 \ll 1$. Considering only the lowest two states [and subtracting out an energy as in Eqs. (33)], we adiabatically eliminate the second state in

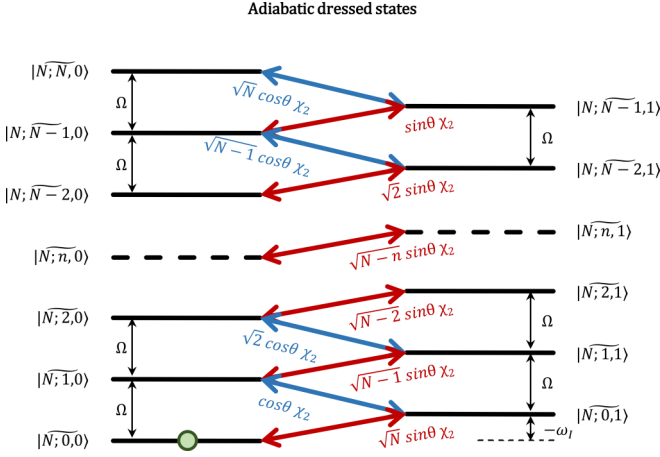


FIG. 11. Fully symmetric collective dressed state levels for adiabatic, time-dependent fields when $\delta_1 + \delta_2 = 0$. In contrast to the constant amplitude dressed ladders, the only state populated initially is the $|N; \widetilde{0}, 0\rangle$ state and the only final states populated are $|N; \widetilde{0}, 0\rangle$ and $|N; \widetilde{0}, 1\rangle$. Although not indicated explicitly, χ_1 , χ_2 , Ω , and θ are functions of time.

the first ladder using

$$\tilde{c}_{10}^{Nd}(t) = -\frac{\chi_2(t) \cos[\theta(t)] \tilde{c}_{01}^{Nd}(t)}{\Omega(t)}, \quad (66)$$

leading to evolution equations for the lower state amplitudes [13]:

$$d\tilde{c}_{00}^{Nd}/dt = -i\sqrt{N} \sin[\theta(t)] \chi_2(t) \tilde{c}_{01}^{Nd}, \quad (67a)$$

$$d\tilde{c}_{01}^{Nd}/dt = -i\sqrt{N} \sin[\theta(t)] \chi_2(t) \tilde{c}_{00}^{Nd} - i \left[(\delta_1 + \delta_2) - \omega_1(t) + \frac{[\chi_2(t) \cos[\theta(t)]]^2}{\Omega(t)} \right] \tilde{c}_{01}^{Nd}. \quad (67b)$$

Equations (67) lead to results that agree with the exact results when $|\delta_1 T_p| \gg 1$. This is true even when the inequalities (7) are violated. There is no modulation at frequency δ_1 in the adiabatic result. For the Gaussian pulse envelope of Eq. (5), in Fig. 12, we plot $|c_{01}^N(\infty)|^2 = |\tilde{c}_{01}^{Nd}(\infty)|^2$ as a function of $\chi_{RN}T/\sqrt{2}$ for $\chi_1 = 30$, $\chi_2 = 2$, $\delta_1 = -\delta_2 = 50$, and

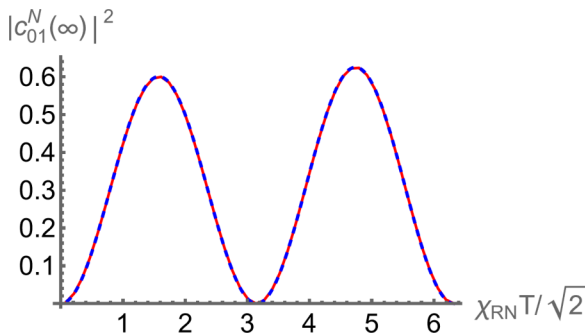


FIG. 12. Graph of $|c_{01}^N(\infty)|^2$ as a function of $\chi_{RN}T/\sqrt{2}$ for $\chi_1 = 30$, $\chi_2 = 2$, $\delta_1 = -\delta_2 = 50$, and $N = 100$. The blue, dashed curve is the adiabatic solution and the red solid curve is the exact solution.

$N = 100$, and compare it with the exact solution. The blue, dashed curve is the adiabatic solution and the red solid curve is the exact solution—as can be seen, they agree perfectly, even though $\chi_1/\delta_1 = 0.6$.

V. EFFECTIVE HAMILTONIAN AND THE HOLSTEIN-PRIMAKOFF TRANSFORMATION

The Hamiltonian that gives rise to the evolution Eqs. (26) is

$$H = \hbar \sum_{n,q} [n\delta_1 + q(\delta_1 + \delta_2)] |N; n, q\rangle \langle N; n, q| + \hbar\chi_1(t) \sum_{n=0}^{N-q+1} \sqrt{n(N-n-q+1)} |N; n, q\rangle \langle N; n-1, q| + \hbar\chi_1(t) \sum_{n=0}^{N-q} \sqrt{(n+1)(N-n-q)} |N; n, q\rangle \langle N; n+1, q| + \hbar\chi_2(t) \sum_{q=0}^{N-n} \sqrt{n(q+1)} |N; n, q\rangle \langle N; n-1, q+1| + \hbar\chi_2(t) \sum_{q=0}^{N-n} \sqrt{q(n+1)} |N; n, q\rangle \langle N; n+1, q-1| \quad (68)$$

and is exact. However, in the limit that $N \gg n, q, 1$, it reduces to

$$H \approx \hbar \sum_{n,q} [n\delta_1 + q(\delta_1 + \delta_2)] |N; n, q\rangle \langle N; n, q| + \hbar\chi_1(t) \sqrt{N} \sum_n (\sqrt{n} |N; n, q\rangle \langle N; n-1, q| + \sqrt{(n+1)} |N; n, q\rangle \langle N; n+1, q|) + \hbar\chi_2(t) \sum_q \left(\sqrt{n(q+1)} |N; n, q\rangle \langle N; n-1, q+1| + \sqrt{q(n+1)} |N; n, q\rangle \langle N; n+1, q-1| \right). \quad (69)$$

This a Hamiltonian for coupled oscillators, in which one of the oscillators is driven by an incident field. That is, if the ladder operators for each oscillator are denoted by a and b , then

$$H \approx \hbar[\delta_1 a^\dagger a + (\delta_1 + \delta_2) b^\dagger b] + \hbar\chi_1(t) \sqrt{N}(a + a^\dagger) + \hbar\chi_2(t)(a^\dagger b + b^\dagger a). \quad (70)$$

Since these correspond to linear oscillators, there can be no nonlinear effects. To simulate the blockade we must truncate the b oscillator. That is, we replace b by $\sigma_- = |1\rangle\langle 3|$, b^\dagger by $\sigma_+ = |3\rangle\langle 1|$, and $b^\dagger b$ by $\sigma_+ \sigma_- = |3\rangle\langle 3| = \sigma_{33}$, yielding

$$H \approx \hbar[\delta_1 a^\dagger a + (\delta_1 + \delta_2) \sigma_{33}] + \hbar\chi_1(t) \sqrt{N}(a + a^\dagger) + \hbar\chi_2(t)(a^\dagger \sigma_- + \sigma_+ a), \quad (71)$$

which corresponds to an oscillator driven by an off-resonant field that is coupled to a two-level atom. The excited state of the “two-level” atom is actually the collective Rydberg state.

The equation of motion for a is

$$\dot{a} = -i\delta_1 a - i\chi_1(t) \sqrt{N} - i\chi_2(t) \sigma_- . \quad (72)$$

The adiabatic solution of this equation is

$$a = -\frac{\chi_1(t)\sqrt{N} + \chi_2(t)\sigma_-}{\delta_1}. \quad (73)$$

Note that the adiabatic solution might fail when $\frac{[\chi_1(t)]^2 T}{\delta_1} > 1$.

The equations for the atomic operators are

$$\dot{\sigma}_{11} = i\chi_2(t)[\sigma_+ a - a^\dagger \sigma_-], \quad (74a)$$

$$\dot{\sigma}_{33} = -i\chi_2(t)[\sigma_+ a - a^\dagger \sigma_-], \quad (74b)$$

$$\dot{\sigma}_+ = i(\delta_1 + \delta_2)\sigma_+ - i\chi_2(t)a^\dagger[\sigma_{33} - \sigma_{11}], \quad (74c)$$

$$\dot{\sigma}_- = -i(\delta_1 + \delta_2)\sigma_- + i\chi_2(t)[\sigma_{33} - \sigma_{11}]a, \quad (74d)$$

where $\sigma_{11} = \sigma_- \sigma_+ = |1\rangle\langle 1|$. If we insert the solution (73) for a in these equations, we find

$$\dot{\sigma}_{11} = -i\frac{\chi_2(t)\chi_1(t)\sqrt{N}}{\delta_1}[\sigma_+ - \sigma_-], \quad (75a)$$

$$\dot{\sigma}_{33} = i\frac{\chi_2(t)\chi_1(t)\sqrt{N}}{\delta_1}[\sigma_+ - \sigma_-], \quad (75b)$$

$$\dot{\sigma}_+ = i(\delta_1 + \delta_2)\sigma_+ + i\frac{\chi_2(t)\chi_1(t)\sqrt{N}}{\delta_1}[\sigma_{33} - \sigma_{11}] - i\frac{[\chi_2(t)]^2}{\delta_1}\sigma_+, \quad (75c)$$

$$\dot{\sigma}_- = (\dot{\sigma}_+)^\dagger. \quad (75d)$$

These equations suggest that there is no level shift associated with the field χ_1 , but this can be traced to the neglect of q in going from Eq. (68) to Eq. (69), under the assumption that $N \gg q$ (see below).

Suppose we want to find corrections to the excited-state population resulting from multiple level 2 excitations. If we want to estimate corrections, we can look only at terms in the Hamiltonian related to the χ_1 field and drop the q terms in the Hamiltonian. In this limit

$$H = \hbar \sum_n n \delta_1 |N; n\rangle\langle N; n| + \hbar \chi_1(t) \sum_{n=0}^{N-q+1} \sqrt{n(N-n+1)} |N; n\rangle\langle N; n-1| + \hbar \chi_1(t) \sum_{n=0}^{N-q} \sqrt{(n+1)(N-n)} |N; n\rangle\langle N; n+1|. \quad (76)$$

We convert this to operators by replacing n by $a^\dagger a$ to arrive at

$$H \approx \hbar \delta_1 a^\dagger a + \hbar \chi_1(t) \sqrt{N} \left[\sqrt{\left(1 - \frac{a^\dagger a}{N}\right)} a + a^\dagger \sqrt{\left(1 - \frac{a^\dagger a}{N}\right)} \right], \quad (77)$$

where we have neglected terms of order $1/N$. This result has essentially the same form as the Holstein-Primakoff (HP) transformation [8]. If we expand to lowest order, then

$$H \sim \hbar \delta_1 a^\dagger a + \hbar \chi_1(t) \sqrt{N} (a + a^\dagger) - \hbar \chi_1(t) \frac{1}{2\sqrt{N}} (a^\dagger a a + a^\dagger a^\dagger a). \quad (78)$$

Including the interaction with the second field,

$$H \approx \hbar \delta_1 a^\dagger a + \hbar \chi_1(t) \sqrt{N} (a + a^\dagger) - \hbar \chi_1(t) \frac{1}{2\sqrt{N}} (a^\dagger a a + a^\dagger a^\dagger a) + \hbar \chi_2(t) (a^\dagger \sigma_- + \sigma_+ a). \quad (79)$$

The equation for \dot{a} is

$$\dot{a} = -i\delta_1 a - i\chi_1(t) \sqrt{N} + i\chi_1(t) \frac{1}{2\sqrt{N}} (a^2 + 2a^\dagger a) - i\chi_2(t) \sigma_- . \quad (80)$$

One possibility is to put the adiabatic solution

$$a = -\frac{\chi_1(t)\sqrt{N} + \chi_2(t)\sigma_-}{\delta_1} \quad (81)$$

in the third term and neglect the $\chi_2(t)\sigma_-$ term. Then

$$\dot{a} \approx -i\delta_1 a - i\chi_1(t) \sqrt{N} \left(1 - \frac{3}{2} \frac{\chi_1^2(t)}{\delta_1^2}\right) - i\chi_2(t) \sigma_- , \quad (82)$$

such that

$$a \approx -\frac{\chi_1(t)\sqrt{N} \left(1 - \frac{3}{2} \frac{\chi_1^2(t)}{\delta_1^2}\right) + \chi_2(t)\sigma_-}{\delta_1}. \quad (83)$$

As a consequence, the coupling is modified as

$$\sqrt{N} \frac{\chi_2(t)\chi_1(t)}{\delta_1} \rightarrow \sqrt{N} \frac{\chi_2(t)\chi_1(t)}{\delta_1} \left(1 - \frac{3}{2} \frac{[\chi_1(t)]^2}{\delta_1^2}\right), \quad (84)$$

consistent with the lowest-order correction to the coupling in the adiabatic model given in Eq. (67).

The use of the HP approximation does not simplify the calculation. However, if the light shifts are negligible, it does provide a simple justification for the two-level model. The Hamiltonian of Eq. (71) can be viewed as the lowest order approximation to the HP transformation. Equation (71) led to Eqs. (75). If the light shifts are neglected in Eqs. (75) and expectation values are taken, one arrives at density-matrix equations consistent with the two-level approximation. In other words, the Heisenberg operator approach of the HP transformation allows one to arrive at expressions for the *total* Rydberg population without regard to the *individual* state populations of the ladder states.

How to include the light shift from the first field

Even with corrections, the Hamiltonian given by Eq. (79) does not contain the light shifts produced by field 1. The reason for this is clear. In the dressed basis, there are two ladders and the $q = 1$ ladder is shifted slightly from the $q = 0$ ladder. There is no analogous term in HP since we have assumed that $N \gg q$; in effect, we treat $q = 0$ and 1 in the same manner. Thus, to include the light shift in HP, we must somehow account for the q dependence. To do so we expand

$$\sqrt{n(N-n-q+1)} \approx \sqrt{nN} - \frac{q\sqrt{n}}{2\sqrt{N}}. \quad (85)$$

As a consequence, the effective Hamiltonian given in Eq. (79) is replaced by

$$H \approx \hbar \left[\delta_1 a^\dagger a + \left(\delta_1 + \delta_2 - \frac{\chi_1(t)(a + a^\dagger)}{2\sqrt{N}} \right) b^\dagger b \right] + \hbar \chi_1(t) \sqrt{N} (a + a^\dagger) + \hbar \chi_2(t) (a^\dagger b + b^\dagger a). \quad (86)$$

If, in lowest approximation for large N , we replace $(a + a^\dagger)$ in the frequency term by

$$(a + a^\dagger) \approx -\frac{2\chi_1(t)\sqrt{N}}{\delta_1}, \quad (87)$$

then the effective Hamiltonian becomes

$$H \approx \hbar \left[\delta_1 a^\dagger a + \left(\delta_1 + \delta_2 + \frac{[\chi_1(t)]^2}{\delta_1} \right) b^\dagger b \right] + \hbar \chi_1(t) \sqrt{N} (a + a^\dagger) + \hbar \chi_2(t) (a^\dagger b + b^\dagger a). \quad (88)$$

We then proceed as before, so that the effective equations for the atomic operators are

$$\dot{\sigma}_{11} = -i \frac{\chi_2(t)\chi_1(t)}{\delta_1} \sqrt{N} [\sigma_+ - \sigma_-], \quad (89a)$$

$$\dot{\sigma}_{33} = i \frac{\chi_2(t)\chi_1(t)}{\delta_1} \sqrt{N} [\sigma_+ - \sigma_-], \quad (89b)$$

$$\dot{\sigma}_+ = i \left(\delta_1 + \delta_2 + \frac{[\chi_1(t)]^2}{\delta_1} \right) \sigma_+ + i \frac{\chi_2(t)\chi_1(t)}{\delta_1} \sqrt{N} [\sigma_{33} - \sigma_{11}] - i \frac{[\chi_2(t)]^2}{\delta_1} \sigma_+, \quad (89c)$$

$$\dot{\sigma}_- = (\dot{\sigma}_+)^\dagger. \quad (89d)$$

Now the light shifts from both fields are included. Moreover, if we also include the corrections to the coupling term given by Eq. (84), the HP and dressed state approaches are in excellent agreement in the limit that inequalities (7) hold.

VI. CONCLUSIONS

We have presented a detailed theory of the Rydberg blockade, including contributions from multiple intermediate-state excitations. It has been shown that a dressed state approach offers distinct advantages when multiple intermediate-state excitations occur. In the case of fixed amplitude fields, the multiple intermediate excitations can result in comblike modulated populations of *individual* states having one Rydberg excitation and $n \ll N$ intermediate-state excitations. How-

ever, when summed over *all* such state populations, most of the modulation disappears and the system is described to a good approximation by an effective two-level model. In the case of adiabatic, pulsed fields, there is no such modulation and an effective two-level model (in the dressed basis), corrected for light shifts, can be used to model the system. The calculation has been restricted to fully symmetric (phased) states containing at most one Rydberg excitation. Spontaneous decay from the intermediate state will couple these states to states outside the symmetric subspace, but such effects are expected to provide only small corrections provided the number of excited states $n \ll N$ and $(\chi_1^2/\delta_1^2)\gamma_2 T \ll 1$. In other words, as was the case for the light shifts, there are no collective decay rates proportional to N that contribute to the signal [14]. In addition to solving this problem using conventional methods, we have shown that similar results could be obtained using a form of the Holstein-Primakoff transformation. Given the state of the art of current experiments involving atoms in lattices, it may be possible to test some of our predictions concerning the role of multiple intermediate excitations.

ACKNOWLEDGMENTS

We would like to thank A. Kuzmich for helpful discussions. This research of P.R.B. and H.N. is supported by the Air Force Office of Scientific Research and the National Science Foundation.

APPENDIX

We can improve upon the lowest-order solution for the dressed state amplitudes by expanding the subspace for n excitations from two to six levels. That is, we look at a truncated subspace for dressed state amplitudes:

$$\mathbf{b}_n^{Nd} = [b_{n0}^{Nd}, b_{n1}^{Nd}, \tilde{b}_{n+1,0}^{Nd}, \tilde{b}_{n+1,1}^{Nd}, \tilde{b}_{n-1,0}^{Nd}, \tilde{b}_{n-1,1}^{Nd}] \quad (A1)$$

with

$$\tilde{b}_{n+1,0}^{Nd} = e^{-i\Omega t} b_{n+1,0}^{Nd}, \quad \tilde{b}_{n+1,1}^{Nd} = e^{-i\Omega t} b_{n+1,1}^{Nd}, \quad (A2a)$$

$$\tilde{b}_{n-1,0}^{Nd} = e^{i\Omega t} b_{n-1,0}^{Nd}, \quad \tilde{b}_{n-1,1}^{Nd} = e^{i\Omega t} b_{n-1,1}^{Nd}. \quad (A2b)$$

We truncate the space by considering *only* these amplitudes, which obey the matrix equation

$$i\hbar \dot{\mathbf{b}}_n^{Nd} = \mathbf{H}_n \mathbf{b}_n^{Nd}, \quad (A3)$$

subject to the initial conditions $\mathbf{b}_n^{Nd}(0) = [b_{n0}^{Nd}(0), 0, b_{n+1,0}^{Nd}(0), 0, b_{n-1,0}^{Nd}(0), 0]$ with

$$H_n = \hbar \begin{pmatrix} 0 & \chi(n, N) & 0 & 0 & 0 & \chi(n) \\ \chi(n, N) & \sigma & \chi(n+1) & 0 & 0 & 0 \\ 0 & \chi(n+1) & \Omega & \chi(n+1, N) & 0 & 0 \\ 0 & 0 & \chi(n+1, N) & \Omega + \sigma & 0 & 0 \\ 0 & 0 & 0 & 0 & -\Omega & \chi(n-1, N) \\ \chi(n) & 0 & 0 & 0 & \chi(n-1, N) & -\Omega + \sigma \end{pmatrix}, \quad (A4)$$

where

$$\begin{aligned}\chi(n, N) &= \chi_2 \sin \theta \sqrt{N-n}, \\ \chi(n) &= \sqrt{n} \chi_2 \cos \theta,\end{aligned}$$

and

$$\sigma = \delta_1 + \delta_2 - \omega_1. \quad (\text{A5})$$

The formal solution of Eq. (A3) is

$$\mathbf{b}_n^{Nd}(t) = e^{-i\mathbf{H}_n t/\hbar} \mathbf{b}_n^{Nd}(0), \quad (\text{A6})$$

which can be evaluated numerically. In this truncated subspace the resulting solution is valid *only* for $b_{n0}^{Nd}(t)$ and $b_{n1}^{Nd}(t)$ and this solution provides an excellent approximation to the exact solution provided

$$\frac{\chi_2}{\delta_1} n \approx \frac{\Omega_1^2 \chi_2}{\delta_1^3} N \ll 1. \quad (\text{A7})$$

In fact, when this inequality holds, a first approximation can be obtained by considering only the $[b_{n0}^{Nd}, b_{n1}^{Nd}]$ subspace. For $N \gg n$, the analytic solution of Eq. (A3) in this limited subspace is

$$b_{n0}^{Nd}(t) = b_{n0}^{Nd}(0) e^{-i\sigma t/2} \cos\left(\frac{\sqrt{4\chi_{RN}^2 + \sigma^2}}{2} t\right) + i b_{n0}^{Nd}(0) e^{-i\sigma t/2} \frac{\sigma}{\sqrt{4\chi_{RN}^2 + \sigma^2}} \sin\left(\frac{\sqrt{4\chi_{RN}^2 + \sigma^2}}{2} t\right), \quad (\text{A8a})$$

$$b_{n1}^{Nd}(t) = i b_{n0}^{Nd}(0) e^{-i\sigma t/2} \frac{2\chi_{RN}}{\sqrt{4\chi_{RN}^2 + \sigma^2}} \sin\left(\frac{\sqrt{4\chi_{RN}^2 + \sigma^2}}{2} t\right). \quad (\text{A8b})$$

In this approximation, the total population P_R in the Rydberg ladder is equal to

$$P_R = \sum_{n=0}^{N-1} |b_{n1}^{Nd}(t)|^2 \approx \sum_{n=0}^N |b_{n1}^{Nd}(t)|^2 = \frac{4\chi_{RN}^2}{4\chi_{RN}^2 + \sigma^2} \sin^2\left(\frac{\sqrt{4\chi_{RN}^2 + \sigma^2}}{2} t\right) \quad (\text{A9})$$

and does not exhibit modulation at frequency δ_1 .

In order to see if P_R can exhibit modulation at frequency δ_1 , we must obtain corrections of order χ_2/δ_1 . An approximate analytic solution to Eq. (A3) can be obtained in the limit that

$$\frac{\chi_1^2}{\delta_1^2} \ll 1, \quad |\sigma| \approx \left| \delta_1 + \delta_2 + \frac{\chi_1^2}{\delta_1^2} \right| \ll \chi_{RN}, \quad N \gg n, \quad (\text{A10})$$

for which

$$\mathbf{H}_n \approx \hbar \begin{pmatrix} 0 & -\chi_{RN} & 0 & 0 & 0 & \sqrt{n}\chi_2 \\ -\chi_{RN} & \sigma & \sqrt{n+1}\chi_2 & 0 & 0 & 0 \\ 0 & \sqrt{n+1}\chi_2 & \delta_1 & -\chi_{RN} & 0 & 0 \\ 0 & 0 & -\chi_{RN} & \delta_1 + \sigma & 0 & 0 \\ 0 & 0 & 0 & 0 & -\delta_1 & -\chi_{RN} \\ \sqrt{n}\chi_2 & 0 & 0 & 0 & -\chi_{RN} & -\delta_1 + \sigma \end{pmatrix}. \quad (\text{A11})$$

To obtain the state amplitudes in this limit, we first use degenerate perturbation theory to diagonalize the (nearly) degenerate $\{b_{n0}^{Nd}, b_{n1}^{Nd}\}$ sub-block. If $\chi_{RN} \gg |\sigma|$, the eigenvectors are then given approximately by

$$|\mu 0\rangle' \approx \frac{1}{\sqrt{2}} (|\mu 0\rangle + |\mu 1\rangle), \quad (\text{A12a})$$

$$|\mu 1\rangle' \approx \frac{1}{\sqrt{2}} (|\mu 0\rangle - |\mu 1\rangle) \quad (\text{A12b})$$

($\mu = n, n \pm 1$) and the transformed matrix is given by

$$\mathbf{H}_n'' \approx \hbar \begin{pmatrix} \frac{\sigma}{2} - \chi_{RN} & 0 & \sqrt{n+1}\frac{\chi_2}{2} & \sqrt{n+1}\frac{\chi_2}{2} & \sqrt{n}\frac{\chi_2}{2} & -\sqrt{n}\frac{\chi_2}{2} \\ 0 & \frac{\sigma}{2} + \chi_{RN} & -\sqrt{n+1}\frac{\chi_2}{2} & -\sqrt{n+1}\frac{\chi_2}{2} & \sqrt{n}\frac{\chi_2}{2} & -\sqrt{n}\frac{\chi_2}{2} \\ \sqrt{n+1}\frac{\chi_2}{2} & -\sqrt{n+1}\frac{\chi_2}{2} & \frac{\sigma}{2} + \delta_1 - \chi_{RN} & 0 & 0 & 0 \\ \sqrt{n+1}\frac{\chi_2}{2} & -\sqrt{n+1}\frac{\chi_2}{2} & 0 & \frac{\sigma}{2} + \delta_1 + \chi_{RN} & 0 & 0 \\ \sqrt{n}\frac{\chi_2}{2} & \sqrt{n}\frac{\chi_2}{2} & 0 & 0 & \frac{\sigma}{2} - \delta_1 - \chi_{RN} & 0 \\ -\sqrt{n}\frac{\chi_2}{2} & -\sqrt{n}\frac{\chi_2}{2} & 0 & 0 & 0 & \frac{\sigma}{2} - \delta_1 + \chi_{RN} \end{pmatrix}. \quad (\text{A13})$$

We now use nondegenerate perturbation theory, assuming that $\delta_1 \gg \chi_{RN}$, to obtain the eigenenergies:

$$E_1'' \approx \hbar(-\chi_{RN} + s), \quad E_2'' \approx \hbar(\chi_{RN} + s), \quad (\text{A14a})$$

$$E_{3n}'' \approx \hbar \left(s + \delta_1 - \chi_{RN} + \frac{(n+2)\chi_2^2}{\delta_1} \right), \quad (\text{A14b})$$

$$E_{4n}'' \approx \hbar \left(s + \delta_1 + \chi_{RN} + \frac{(n+2)\chi_2^2}{\delta_1} \right), \quad (\text{A14c})$$

$$E_{5n}'' \approx \hbar \left(s - \delta_1 - \chi_{RN} - \frac{(n-1)\chi_2^2}{\delta_1} \right), \quad (\text{A14d})$$

$$E_{6n}'' \approx \hbar \left(s - \delta_1 + \chi_{RN} - \frac{(n-1)\chi_2^2}{\delta_1} \right), \quad (\text{A14e})$$

where

$$s = \frac{\chi_1^2}{2\delta_1} - \frac{\chi_2^2}{2\delta_1} + \frac{\delta_1 + \delta_2}{2}. \quad (\text{A15})$$

The eigenkets associated with these eigenenergies are given approximately by [15]

$$|n0\rangle'' \approx |n0\rangle' \approx \frac{1}{\sqrt{2}}(|n0\rangle + |n1\rangle), \quad (\text{A16a})$$

$$|n1\rangle'' \approx |n1\rangle' \approx \frac{1}{\sqrt{2}}(|n0\rangle - |n1\rangle), \quad (\text{A16b})$$

$$\begin{aligned} |n+1, 0\rangle'' &\approx |n+1, 0\rangle' + \sqrt{n+1} \frac{\chi_2}{2\delta_1} (|n0\rangle' - |n1\rangle') \\ &= \frac{1}{\sqrt{2}}(|n+1, 0\rangle + |n+1, 1\rangle) + \sqrt{n+1} \frac{\chi_2}{\sqrt{2}\delta_1} |n1\rangle, \end{aligned} \quad (\text{A16c})$$

$$\begin{aligned} |n+1, 1\rangle'' &\approx |n+1, 1\rangle' + \sqrt{n+1} \frac{\chi_2}{2\delta_1} (|n0\rangle' - |n1\rangle') \\ &= \frac{1}{\sqrt{2}}(|n+1, 0\rangle - |n+1, 1\rangle) + \sqrt{n+1} \frac{\chi_2}{\sqrt{2}\delta_1} |n1\rangle, \end{aligned} \quad (\text{A16d})$$

$$\begin{aligned} |n-1, 0\rangle'' &\approx |n-1, 0\rangle' - \sqrt{n} \frac{\chi_2}{2\delta_1} (|n0\rangle' + |n1\rangle') \\ &= \frac{1}{\sqrt{2}}(|n-1, 0\rangle + |n-1, 1\rangle) - \sqrt{n} \frac{\chi_2}{\sqrt{2}\delta_1} |n0\rangle, \end{aligned} \quad (\text{A16e})$$

$$\begin{aligned} |n-1, 1\rangle'' &\approx |n-1, 1\rangle' + \sqrt{n} \frac{\chi_2}{2\delta_1} (|n0\rangle' + |n1\rangle') \\ &= \frac{1}{\sqrt{2}}(|n-1, 0\rangle - |n-1, 1\rangle) + \sqrt{n} \frac{\chi_2}{\sqrt{2}\delta_1} |n0\rangle. \end{aligned} \quad (\text{A16f})$$

The state vector $|\psi(t)\rangle$ in this subspace is expanded as

$$\begin{aligned} |\psi(t)\rangle &= [b_{n0}^{Nd}(0)]'' e^{i\chi_{RN}t} e^{-ist} |n0\rangle'' + [b_{n1}^{Nd}(0)]'' e^{-i\chi_{RN}t} \\ &\quad \times e^{-ist} |n1\rangle'' + [b_{n+1,0}^{Nd}(0)]'' e^{-i\delta_1 t} |n+1, 0\rangle'' \end{aligned}$$

$$\begin{aligned} &+ [b_{n+1,1}^{Nd}(0)]'' e^{-i\delta_1 t} |n+1, 1\rangle'' + [b_{n-1,0}^{Nd}(0)]'' \\ &\quad \times e^{i\delta_1 t} |n-1, 0\rangle'' + [b_{n-1,1}^{Nd}(0)]'' e^{i\delta_1 t} |n-1, 1\rangle''. \end{aligned} \quad (\text{A17})$$

Using the fact that

$$[b_{n0}^{Nd}(0)]'' \approx \frac{1}{\sqrt{2}} b_{n0}^{Nd}(0) - \sqrt{n+1} \frac{\chi_2}{\sqrt{2}\delta_1} b_{n+1,0}^{Nd}(0), \quad (\text{A18a})$$

$$[b_{nn}^{Nd}(0)]'' \approx \frac{1}{\sqrt{2}} b_{nn}^{Nd}(0) + \sqrt{n+1} \frac{\chi_2}{\sqrt{2}\delta_1} b_{n+1,0}^{Nd}(0), \quad (\text{A18b})$$

$$[b_{n+1,0}^{Nd}(0)]'' \approx \frac{1}{\sqrt{2}} b_{n+1,0}^{Nd}(0); \quad [b_{n+1,1}^{Nd}(0)]'' \approx \frac{1}{\sqrt{2}} b_{n+1,0}^{Nd}(0), \quad (\text{A18c})$$

$$[b_{n-1,0}^{Nd}(0)]'' \approx \frac{1}{\sqrt{2}} b_{n-1,0}^{Nd}(0); \quad [b_{n-1,1}^{Nd}(0)]'' \approx \frac{1}{\sqrt{2}} b_{n-1,0}^{Nd}(0), \quad (\text{A18d})$$

we find the state amplitudes:

$$\begin{aligned} b_{n0}^{Nd}(t) &\approx b_{n0}^{Nd}(0) e^{-ist} \cos(\chi_{RN}t) - ib_{n+1,0}^{Nd}(0) e^{-ist} \frac{\chi_2}{\delta_1} \sqrt{n+1} \\ &\quad \times \sin(\chi_{RN}t) - ib_{n-1,0}^{Nd}(0) \frac{\chi_2}{\delta_1} \sqrt{n} e^{i\delta_1 t} e^{-ist} \sin(\chi_{RN}t), \end{aligned} \quad (\text{A19a})$$

$$\begin{aligned} b_{n1}^{Nd}(t) &\approx ib_{n0}^{Nd}(0) e^{-ist} \sin(\chi_{RN}t) \\ &\quad + b_{n+1,0}^{Nd}(0) \frac{\chi_2}{\delta_1} \sqrt{n+1} (e^{-i\delta_1 t} - 1) e^{-ist} \cos(\chi_{RN}t). \end{aligned} \quad (\text{A19b})$$

In writing these equations, we have neglected contributions from the light shifts of field 2 in the correction terms of order χ_2/δ_1 . It then follows that the total Rydberg population,

$$\begin{aligned} P_R &\approx \sum_{n=0}^N |b_{n1}^{Nd}(t)|^2 \approx \sin^2(\chi_{RN}t) \\ &\quad - \frac{\chi_2}{\delta_1} \sin(\delta_1 t) \sin(2\chi_{RN}t) \sum_{n=0}^N \sqrt{n+1} b_{n0}^{Nd}(0) b_{n+1,0}^{Nd}(0), \end{aligned} \quad (\text{A20})$$

exhibits modulation at frequency δ_1 , with a modulation depth of order χ_2/δ_1 . For $(\chi_1/\delta_1)^2 \ll 1$ and $N \gg 1$,

$$\sum_{n=0}^N \sqrt{n+1} b_{n0}^{Nd}(0) b_{n+1,0}^{Nd}(0) \approx 2 \frac{\chi_1}{\delta_1} \sqrt{N}. \quad (\text{A21})$$

- [1] M. D. Lukin, M. Fleischhauer, R. Cote, L. M. Duan, D. Jaksch, J. I. Cirac, and P. Zoller, *Phys. Rev. Lett.* **87**, 037901 (2001).
 [2] See, for example, E. Urban, T. A. Johnson, T. Henage, L. Isenhower, D. D. Yavuz, T. G. Walker, and M. Saffman, *Nat. Phys.* **5**, 110 (2009); A. Gaëtan, Y. Miroshnychenko, T. Wilk, A. Chotia, M. Viteau, D. Comparat, P. Pillet, A. Browaeys, and P. Grangier, *ibid.* **5**, 115 (2009).

- [3] See, for example, D. Tong, S. M. Farooqi, J. Stanojevic, S. Krishnan, Y. P. Zhang, R. Côté, E. E. Eyler, and P. L. Gould, *Phys. Rev. Lett.* **93**, 063001 (2004); K. Singer, M. Reetz-Lamour, T. Amthor, L. G. Marcassa, and M. Weidemüller, *ibid.* **93**, 163001 (2004); T. Cubel Liebisch, A. Reinhard, P. R. Berman, and G. Raithel, *ibid.* **95**, 253002 (2005); R. Heidemann, U. Raitzsch, V. Bendkowsky, B. Butscher, R. Löw,

- L. Santos, and T. Pfau, *ibid.* **99**, 163601 (2007); Y. O. Dudin, L. Li, F. Bariani, and A. Kuzmich, *Nat. Phys.* **8**, 790 (2012); J. Zeiher, P. Schauß, S. Hild, T. Macrì, I. Bloch, and C. Gross, *Phys. Rev. X* **5**, 031015 (2015); C. Qiao, C. Tan, J. Siegl, F. Hu, Z. Niu, Y. Jiang, M. Weidemüller, and B. Zhu, *Phys. Rev. A* **103**, 063313 (2021).
- [4] R. H. Dicke, *Phys. Rev.* **93**, 99 (1954).
- [5] N. Shammah, S. Ahmed, N. Lambert, S. De Liberato, and F. Nori, *Phys. Rev. A* **98**, 063815 (2018).
- [6] For reviews of this subject, see D. Comparat and P. Pillet, *J. Opt. Soc. Am. B* **27**, A208 (2010); A. Browaeys and T. Lahaye, *Nat. Phys.* **16**, 132 (2020).
- [7] Some authors have examined how decay of the intermediate state modifies the Rydberg dynamics, but using approaches very different than the one that we use. See C. Ates, T. Pohl, T. Pattard, and J. M. Rost, *Phys. Rev. A* **76**, 013413 (2007); R. V. Skannrup, T. v Weerden, Y. vd Werf, T. Johri, E. J. D. Vredenburg, and S. J. J. M. F. Kokkelmans, *J. Phys. B: At. Mol. Opt. Phys.* **53**, 084008 (2020), and references therein.
- [8] T. Holstein and H. Primakoff, *Phys. Rev.* **58**, 1098 (1940).
- [9] The decay rate is essentially that associated with the Rabi oscillations of a single atom.
- [10] P. R. Berman and V. S. Malinovsky, *Principles of Laser Spectroscopy and Quantum Optics* (Princeton University, Princeton, NJ, 2011), Chap. 2.
- [11] Even though $N \gg 1$ and $N \gg n_2$ it would be a mistake to replace $\sqrt{N-1}$ by \sqrt{N} in Eq. (31b). If we did so, we would miss the light shift associated with field 1. A similar feature arises in our discussion of the Holstein-Primakoff transformation.
- [12] It can be shown that the branching ratio for decay from level $(n, 0)$ to $(n-1, 0)$ is $(N-n+1)/N$ and for decay from level $(n, 1)$ to $(n-1, 1)$ is $(N-n)/N$. Therefore, if $N \gg 1$ and if the number of intermediate-state excitations is much less than N , most of the decay is confined to the fully symmetric states.
- [13] See D. Jaksch, J. I. Cirac, P. Zoller, S. L. Rolston, R. Côté, and M. D. Lukin, *Phys. Rev. Lett.* **85**, 2208 (2000), which points out the advantage of using adiabatic states in the two-atom, two state model.
- [14] We have run some simulations including decay that confirm that the Rabi oscillations are not damped at a rate proportional to N , even when there are many intermediate-state excitations; however, decay *can* wash out some of the modulation of the total Rydberg population.
- [15] For the Hamiltonian given by Eq. (A13) nondegenerate perturbation theory can be used to obtain the third through sixth eigenkets, but not the first and second when χ_2 is comparable with χ_{RN} ; see P. Berman, *Introductory Quantum Mechanics* (Springer, New York, 2018), Sec. 14.2). Thus, in estimating the state amplitudes we miss a term of order χ_2/δ_1 that displaces the state amplitudes but is not modulated at frequency δ_1 . This explains the discrepancy between the approximate and exact solutions seen in Fig. 10. Note, however, that Eqs. (A19) conserve probability to order χ_2/δ_1 . If $\chi_2/\delta_1 \ll 1$, we found that a somewhat better approximation is obtained if the $\sin^2(\chi_{RN}t)$ term in Eq. (A20) is replaced by $\sin^2(\chi_{RN}t)(1 - \frac{N\chi_2\chi_1^2}{6\delta_1^3})$.